

Nonpeptidic Tetrafluorophenoxymethyl Ketone Cruzain Inhibitors as Promising New Leads for Chagas Disease Chemotherapy[†]

Katrien Brak,[‡] Iain D. Kerr,[§] Kimberly T. Barrett,[‡] Nobuhiro Fuchi,[‡] Moumita Debnath,[§] Kenny Ang,^{||} Juan C. Engel,^{||} James H. McKerrow,^{||} Patricia S. Doyle,^{*,||} Linda S. Brinen,^{*,§} and Jonathan A. Ellman^{*,‡}

[‡]Department of Chemistry, University of California, Berkeley, California 94720-1460, [§]Department of Cellular and Molecular Pharmacology, University of California, San Francisco, California 94158-2330, and ^{||}Department of Pathology, UCSF, San Francisco, California 94158-2330

Received November 4, 2009

A century after discovering that the *Trypanosoma cruzi* parasite is the etiological agent of Chagas disease, treatment is still plagued by limited efficacy, toxicity, and the emergence of drug resistance. The development of inhibitors of the major *T. cruzi* cysteine protease, cruzain, has been demonstrated to be a promising drug discovery avenue for this neglected disease. Here we establish that a nonpeptidic tetrafluorophenoxymethyl ketone cruzain inhibitor substantially ameliorates symptoms of acute Chagas disease in a mouse model with no apparent toxicity. A high-resolution crystal structure confirmed the mode of inhibition and revealed key binding interactions of this novel inhibitor class. Subsequent structure-guided optimization then resulted in inhibitor analogues with improvements in potency despite minimal or no additions in molecular weight. Evaluation of the analogues in cell culture showed enhanced activity. These results suggest that nonpeptidic tetrafluorophenoxymethyl ketone cruzain inhibitors have the potential to fulfill the urgent need for improved Chagas disease chemotherapy.

Introduction

Chagas disease, also known as American trypanosomiasis, results from infection by the *Trypanosoma cruzi* parasite. It is estimated that 15 million people are infected with the parasite, resulting in more than 12000 deaths each year.¹ Chagas disease is the leading cause of cardiomyopathy in Latin America.² Current treatment consists of nitroaromatic drugs that are not only toxic but also ineffective for the chronic stage of the disease.^{3,4} These limitations of the existing drugs along with emerging resistance have provided considerable impetus for the development of novel chemotherapy for Chagas disease.^{5,6} One approach consists of developing inhibitors of cruzain, the primary cysteine protease expressed by *T. cruzi*⁷ during infection.^{7–9} Cruzain, a cysteine protease of the papain-like family, plays a vital role at every stage of the parasite's life cycle; it is involved in protein degradation for nutrition, host cell remodeling, and evasion of host defense mechanisms.¹⁰

Vinyl sulfone **1**, a peptidic irreversible inhibitor of cruzain, has been shown to cure parasitic infections in both cell and animal models (Figure 1).^{11–14} While inhibitor **1** is effective, it is peptidic and consequently exhibits low oral bioavailability

and a short circulating half-life.^{15,16} With this in mind, we recently applied the substrate activity screening method to cruzain to obtain novel and potent entirely nonpeptidic inhibitors.^{17,18} In particular, the 1,2,3-triazole-based tetrafluorophenoxymethyl ketone irreversible inhibitor **2** was found to completely eradicate the *T. cruzi* parasite in cell culture (Figure 1). In addition to the nonpeptidic nature of inhibitor **2**, the tetrafluorophenoxymethyl ketone functionality represents a very promising mechanism-based pharmacophore due to its high selectivity for cysteine protease inhibition,^{19–21} as well as the lack of toxicity in animal studies, which was established for a tetrafluorophenoxymethyl ketone-based caspase inhibitor that has entered phase II clinical trials.²²

Herein we report an initial evaluation of inhibitor **2** in a mouse model of Chagas disease. The promising results from these animal studies motivated further development of the tetrafluorophenoxymethyl ketone class of cruzain inhibitors. A high resolution X-ray crystal structure of **2** complexed to cruzain provided characterization of the binding mode of **2** and enabled the design of inhibitors that are approximately 4-fold more potent in addition to having more desirable physicochemical properties. The nonpeptidic nature of these compounds, coupled with their efficacy in cell-culture and mice, makes this class of inhibitors promising candidates for improved chemotherapy for Chagas disease.

Chemistry

The synthesis of 1,4-disubstituted-1,2,3-triazole cruzain inhibitor analogues **3** with differing R1 and R2 substituents required the preparation of various aryloxymethyl ketone azide and quinoline propargyl amine intermediates

[†]Data for the X-ray crystal structure of cruzain complexed to inhibitor **2** has been deposited in the Protein Data Bank (PDB ID 3IUT).

*To whom correspondence should be addressed. For chemistry (J.A.E.): phone, 510-642-4488; fax, 510-642-8369; E-mail, jellman@uclink.berkeley.edu. For X-ray crystallography (L.S.B.): phone, 415-514-3426; fax, 415-502-8193; E-mail, brinen@cmp.ucsf.edu. For biological studies (P.S.D.): phone, 415-476-0825; fax, 415-502-8193; E-mail, patricia.doyle-engel@ucsf.edu.

[‡]Abbreviations: *T. cruzi*, *Trypanosoma cruzi*; IC₅₀, concentration of inhibitor resulting in 50% inhibition; bid, twice daily; *k*_{inact}/*K*_i, second-order inactivation rate constant.

(Scheme 1). The bromomethyl ketone azides **4a–c** were obtained via a three-step, one-pot procedure from the corresponding azido acids by preparation of the isobutyl mixed anhydride, addition of diazomethane to form a diazomethyl ketone, and final treatment with hydrobromic acid. Displacement of the bromide by 2,3,5,6-tetrafluorophenol afforded aryloxymethyl ketone azide intermediates **5a–c**. Enantiomerically pure propargyl amine intermediates **7a–f** were prepared by a two-step reductive amination of quinoline-6-carboxyaldehyde with tertiary carbinamines **6a–f**. 1,4-Disubstituted-1,2,3-triazole inhibitor analogues **3a–i** were then synthesized via a regioselective Cu(I)-catalyzed 1,3-dipolar cycloaddition. Formation of the triazole in the final step enabled the rapid synthesis of a variety of inhibitors

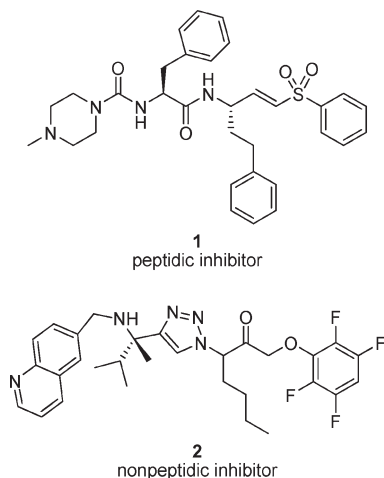
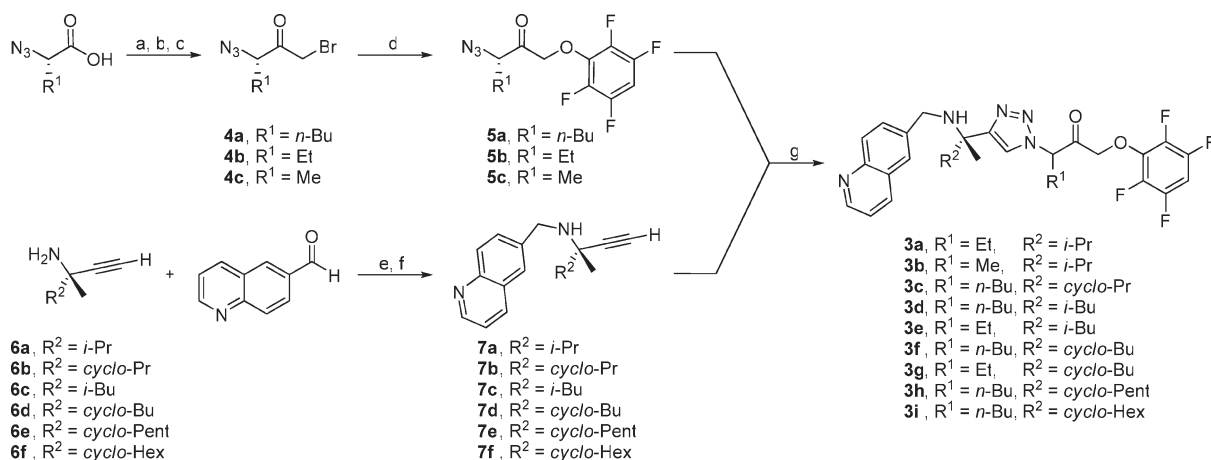


Figure 1. Structures of potent irreversible cruzain inhibitors: dipeptidyl vinyl sulfone **1** and 1,2,3-triazole-based tetrafluorophenoxy-methyl ketone **2**.

Scheme 1. Synthesis of 1,4-Disubstituted-1,2,3-triazole Cruzain Inhibitor Analogues^a



^a Reagents: (a) isobutyl chloroformate, *N*-methylmorpholine, THF, -40 °C; (b) diazomethane, THF, 0 °C; (c) HBr, THF, 0 °C; (d) 2,3,5,6-tetrafluorophenol, KF, DMF, 0 °C; (e) 4 Å molecular sieves, toluene, rt; (f) NaBH₄, MeOH, 0 °C; (g) sodium ascorbate, CuSO₄, 1:1 H₂O:*t*-BuOH, rt.

Table 1. Treatment of *T. cruzi*-Infected C3H Mice with Tetrafluorophenoxy-methyl Ketone Inhibitor **2**

group	no. of mice	dose	acute Chagas disease symptoms	no. of mice without <i>T. cruzi</i> in tissues ^{a, b}	no. of mice with negative hemoculture ^{a, c}
untreated mice	3	none	ascites, paralysis of hind legs, malaise	0	0
treated mice	5	20 mg/kg bid for 27 days via ip	none	2	2 ^d

^a Mice were sacrificed 77 days postinfection. ^b Tissue analysis of sacrificed animals established the absence/presence of *T. cruzi*. ^c *T. cruzi* was cultured from heart blood collected when animals were sacrificed. ^d Hemocultures were performed for 4/5 mice.

resulting from various combinations of the azide and alkyne intermediates.

Results and Discussion

Evaluation in a Mouse Model of Chagas Disease. Mice infected with a large inoculum of *T. cruzi* parasites (1.2×10^6 trypomastigotes) were treated for 27 days with tetrafluorophenoxy-methyl ketone inhibitor **2** (Table 1). The treatment consisted of 20 mg/kg inhibitor **2** in two daily doses via intraperitoneal injection. The mice were monitored for a total of 77 days, at which point they were sacrificed for hemoculture and histopathology. Throughout the experiment, the untreated control mice showed signs of Chagas disease such as ascites (abdominal swelling), malaise, weakness of the hind legs, and ruffled hair. Hemoculture and histopathology revealed that all the untreated mice had positive hemocultures and significant inflammation and infection in heart and skeletal muscle tissue. The mice treated with inhibitor **2**, on the other hand, looked completely normal when sacrificed 77 days postinfection. Importantly, the treatment was well-tolerated by all the mice with no apparent signs of toxicity. Two out of four mice had negative hemocultures, implying animals had no detectable blood parasitemia. Significantly, histopathology revealed that two out of five mice had no inflammation in heart muscle. All the treated mice did show some inflammation in skeletal muscle suggestive of cryptic infection.

The substantial amelioration of acute Chagas disease symptoms is highly significant because, outside of vinyl sulfone **1**, there are no other published reports of successful treatment of Chagas disease with inhibitors of cysteine proteases in animal models.^{12,14} An alternative treatment regimen with **2** or treatment with a more potent analogue could lead to a complete cure of *T. cruzi* infected mice.

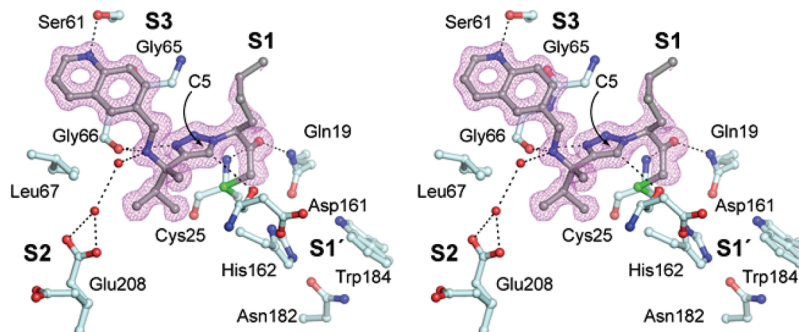


Figure 2. Crystal structure of the cruzain·2 complex (PDB ID 3IUT) elucidates the binding mode of 2 in the cruzain substrate-binding site. Cruzain residues are colored pale cyan and the inhibitor is colored gray. The unbiased $mF_o - DF_c$ electron density for the inhibitor is shown in violet, contoured at the 3σ level. Black dashed lines indicate hydrogen bond interactions between inhibitor 2 and amino acid residues in cruzain's catalytic pocket. The C(5) of the 1,2,3-triazole ring is labeled.

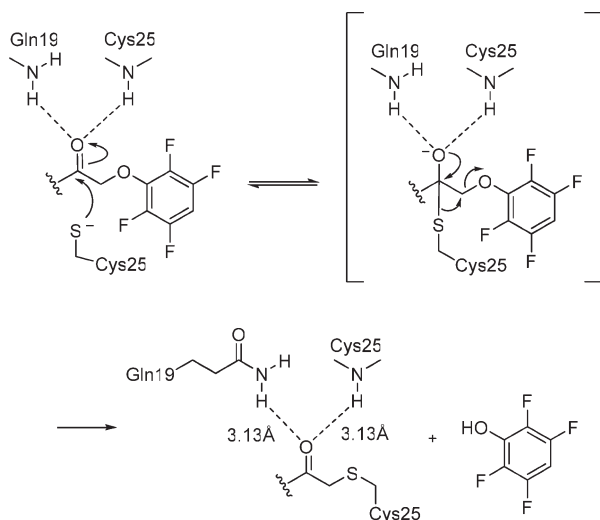


Figure 3. Proposed mechanism of inhibition for tetrafluorophenoxy-methyl ketone inhibitor 2.

For this reason, a structure-guided design of second-generation inhibitors was carried out.

Structural Insight Provided by the X-ray Crystal Structure. The X-ray crystal structure of 2 complexed to cruzain verified both the mode of binding and inactivation (PDB ID 3IUT). Inhibitor 2 is bound in the general orientation that was previously predicted by superimposition with a structure of the homologous protein cathepsin S in complex with a triazole inhibitor that is structurally similar to 2 (PDB ID 2H7J).^{17,23} In particular, the *n*-butyl group is located in the S1 subsite, the methyl and isopropyl functionalities in the S2 subsite, and the quinoline ring in the S3 subsite (Figure 2).

The specific binding interactions between cruzain and inhibitor 2 were elucidated by the high-resolution X-ray crystal structure of cruzain·2. While aryloxymethyl ketone inhibitors are well-studied as caspase inhibitors,^{24,25} this pharmacophore has not been structurally visualized for cruzain or any members of the papain superfamily. The proposed mechanism of inhibition of cysteine proteases by activated ketones involves nucleophilic attack of the cysteine thiolate on the carbonyl carbon, leading to the formation of a tetrahedral intermediate stabilized by the oxyanion hole (Figure 3).^{21,25} Breakdown of the tetrahedral intermediate then results in a displacement of the leaving group and hence irreversible inhibition. The crystal structure reveals that the thiol nucleophile of the active site Cys25 has effectively displaced the

tetrafluorophenoxy moiety of the inhibitor. Taking into account the high resolution of the data, there was no need to include a specific restraint on the C·S γ distance while ensuring overall good geometry for the model. As a result, the distance refines to 1.83 Å, indicating the formation of a covalent bond between Cys25 and the inhibitor. The pharmacophore is further stabilized in the S1' subsite through the formation of hydrogen bonds with the peptide amide of Cys25 (3.13 Å) and N ϵ 2 of Gln19 (3.13 Å) (Figure 2).

A common feature of cruzain-small molecule structures is hydrogen bonding with Gly66, stabilizing the inhibitor in the substrate-binding cleft.^{26–30} In the cruzain·2 complex, Gly66 forms a hydrogen bond with both the amine functionality of the inhibitor (2.85 Å) and the N(3) atom of the 1,2,3-triazole of the inhibitor (3.20 Å) (Figure 2). The strong dipole moment of 1,2,3-triazole rings polarize the C(5) proton to such a degree that it can function as a hydrogen-bond donor.^{31–34} Indeed, the hydrogen bond commonly observed with the backbone carbonyl of Asp161 and amide protons of small molecules is also observed with the C(5) proton of the triazole of inhibitor 2 (3.41 Å) (Figure 2). Because of the ability of 1,2,3-triazoles to function as rigid linking units that mimic the atom placement and electronic properties of a peptide bond without the susceptibility of hydrolysis, many known 1,2,3-triazoles possess biological activity.³⁵

Prior development of this inhibitor class focused on optimizations of interactions in the S3 subsite.¹⁷ Planar heterocycles were introduced to provide hydrophobic interactions with the hydrophobic residues of the pocket. Nitrogen or oxygen heteroatoms were also positioned in the heterocycle to take advantage of potential hydrogen-bonding interactions with the serine residue present in the S3 pocket. A quinoline substituent was found to provide the greatest binding affinity. The crystal structure illustrates that efficient binding is aided by the formation of a hydrogen bond between the quinoline nitrogen and Ser61 (2.79 Å), in addition to nonpolar interactions of the quinoline with Gly65 and Leu67 in the S3 subsite (Figure 2). Additional nonpolar interactions also contribute toward binding, with the isopropyl moiety stabilized by Leu67 and the P2 methyl substituent stabilized by nonpolar regions of Asp161 oriented toward the inhibitor.

The residue at the bottom of the S2 subsite is of particular interest as it is crucial in determining the substrate specificity of papain family cysteine proteases.³⁰ With flexible Glu208 at this position, cruzain has evolved an S2 subsite that is able to tolerate both basic and hydrophobic residues.

An interesting feature of the cruzain·**2** crystal structure is the dual conformation of Glu208. In the crystallized complex, one conformer points toward the inhibitor and interacts with the amine functionality via two bridging water molecules (Figure 2). A second conformer adopts a solvent-exposed orientation, pointing out of the S2 subsite and into a nearby solvent channel in the crystal. We were surprised to discover that the latter appears to interact with a transient and low occupancy second copy of **2** in a solvent channel of the crystal (Figure 4). As the occupancy of the atoms appear low (only the N-terminal portion is partially visible) and we were unable to unequivocally assign atomic positions for all atoms in the molecule, we have not included this second inhibitor molecule in the final coordinates. Of import for this study, while polar interactions with residues lining the solvent channel are possible with this second molecule copy, there is no evidence of covalent bond formation with the pharmacophore, in sharp contrast to what is experimentally observed in the active site bound copy of **2**.

The stereocenter α to the aryloxymethyl ketone moiety is configurationally unstable with complete racemization

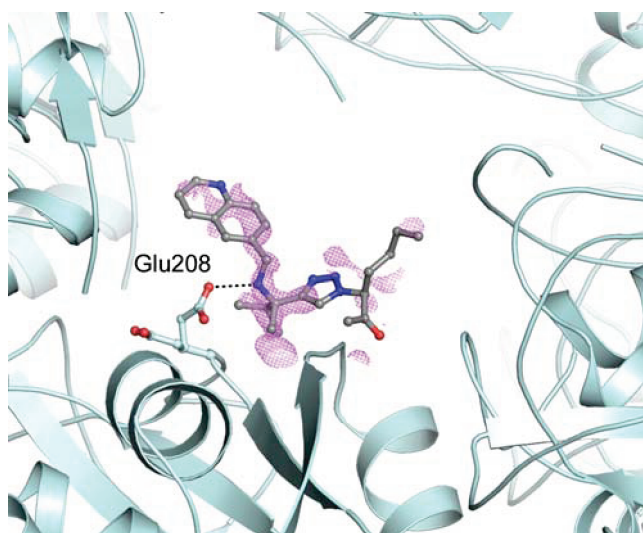


Figure 4. Putative position of a second inhibitor **2** molecule, bound at low occupancy in a solvent channel. Cruzain is colored pale cyan and the inhibitor gray. The unbiased $mF_o - DF_c$ electron density for the inhibitor is shown in violet, contoured at the 3σ level.

within 3 h under the assay conditions (pH = 6.3, 37 °C).¹⁷ The P1 *n*-butyl substituent is less ordered than the rest of the inhibitor and, accordingly, the B-factors in this region are higher in comparison to the rest of the small molecule. However, the crystal structure clearly establishes binding of the epimer with the *S*-configuration at the alpha stereocenter (Figure 2).

Comparison of Cruzain·Nonpeptidic Inhibitor Structures.

The coauthors recently determined the first crystal structure of a nonpeptidic cruzain inhibitor, **8**, complexed to cruzain (PDB ID 3HD3).³⁶ Least-squares superimposition with the cruzain·**2** complex matches 215 C α positions with root-mean-square distances (rmsd) of 0.36 Å (3HD3, monomer A) and 214 C α positions with root-mean-square distances (rmsd) of 0.42 Å (3HD3, monomer B). Inhibitor **8** is a moderately potent cruzain inhibitor ($k_{\text{inact}}/K_i = 6020 \pm 820 \text{ s}^{-1} \text{ M}^{-1}$) that carries the well-characterized vinyl sulfone warhead at the P1' position (Figure 5a). Irreversible inhibition of cruzain is achieved by a Michael addition of the active site thiolate to the β -carbon of the unsaturated vinyl group of the inhibitor. The P2 and P3 substituents (cyclohexane and chlorophenyl, respectively) differ in comparison with **2**; however, both inhibitors are capable of establishing non-polar interactions at these positions with residues lining the binding sites. Interestingly, both inhibitors share the *n*-butyl group at the P1 position, and while this moiety is more flexible than the other substituents in **2**, the *n*-butyl moiety in **8** is well-ordered and unambiguous in the electron density.

Superimposition of the two models shows that inhibitor **2** is able to form polar interactions missing in the complex with vinyl sulfone **8**: specifically, the amine-Gly66 and quinoline-Ser61 hydrogen bonds as well as the amine-Glu208 indirect interaction through two bridging water molecules (Figure 5b). The favorable binding resulting from these interactions is likely the reason for the greater potency of inhibitor **2** ($k_{\text{inact}}/K_i = 157000 \pm 20000 \text{ s}^{-1} \text{ M}^{-1}$). The amide of inhibitor **8** forms a hydrogen bond with the backbone carbonyl of Asp161, an interaction that is replaced in **2** by the C(5) hydrogen of the 1,2,3-triazole ring. With vinyl sulfone **8** lying deeper in the substrate-binding cleft, the *n*-butyl group is able to form nonpolar contacts with Gly23 that are not present in **2**. Therefore, long alkyl functionalities at P1 may not be desirable for the aryloxymethyl ketone cruzain inhibitors. Indeed, only a modest reduction in k_{inact}/K_i is seen when the *n*-butyl is replaced by an ethyl in **3a** (Table 2)

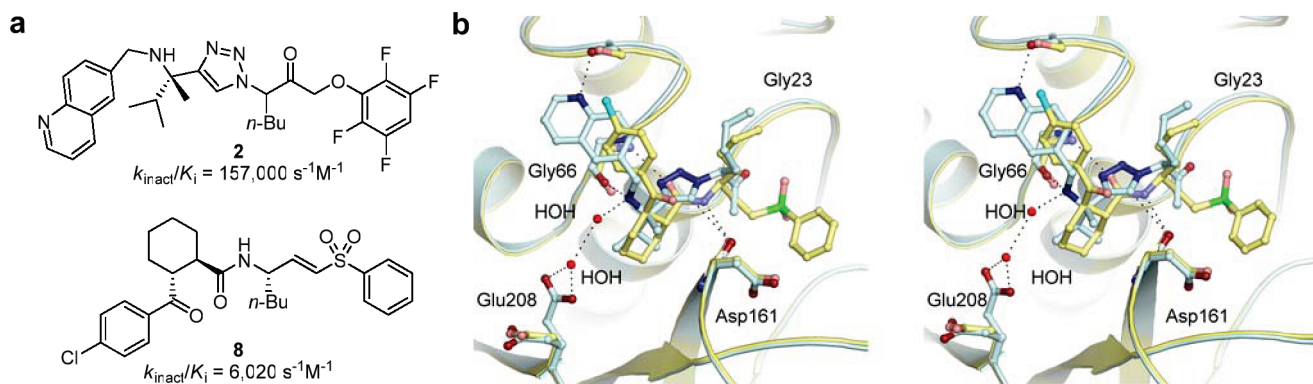
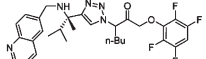
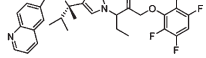
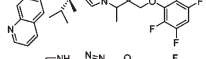
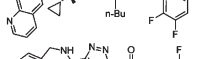
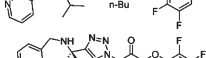
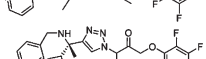
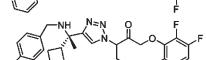
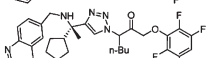
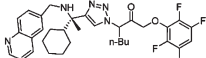
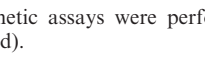


Figure 5. Structural comparison of nonpeptidic inhibitors **2** and **8**. (a) Chemical structures and second-order inactivation constants of tetrafluorophenoxymethyl ketone inhibitor **2** and vinyl sulfone inhibitor **8**. (b) A superimposition of cruzain·**2** (PDB ID 3IUT) and cruzain·**8** (PDB ID 3HD3) crystal structures. The cruzain·**2** complex is colored pale cyan, while the cruzain·**8** complex is colored yellow. Black dashed lines indicate hydrogen bond interactions between the inhibitors and amino acid residues in cruzain's catalytic pocket.

Table 2. Inhibition Kinetics of Tetrafluorophenoxymethyl Ketone Inhibitors Against Cruzain

compd	structure	k_{inact}/K_i ($\text{M}^{-1}\text{s}^{-1}$) ^a	K_i (μM)	k_{inact} (s^{-1})
2		$157,000 \pm 20,000$	0.46 ± 0.4	0.037 ± 0.014
3a		$124,000 \pm 14,000$	1.04 ± 0.45	0.066 ± 0.026
3b		$12,300 \pm 900$	6.76 ± 0.99	0.043 ± 0.004
3c		$179,000 \pm 4,000$	0.94 ± 0.3	0.089 ± 0.030
3d		$657,000 \pm 40,000$	0.10 ± 0.03	0.036 ± 0.011
3e		$487,000 \pm 38,000$	0.19 ± 0.12	0.048 ± 0.029
3f		$680,000 \pm 81,000$	0.13 ± 0.06	0.047 ± 0.019
3g		$522,000 \pm 46,000$	0.35 ± 0.08	0.096 ± 0.026
3h		$432,000 \pm 45,000$	0.11 ± 0.03	0.025 ± 0.004
3i		$58,000 \pm 8,000$	1.22 ± 0.39	0.037 ± 0.011

^a Kinetic assays were performed at least in triplicate (SD values included).

(vide infra), suggesting that the additional two atoms do not contribute appreciably to inhibitor potency.

Structure-Guided Design of Inhibitor Analogues. The crystal structure allowed for the design of analogues that take advantage of the specific contours of the hydrophobic regions of the S1 and S2 pockets. Numerous studies on cruzain substrates and inhibitors have established that a variety of unbranched P1 residues are accommodated because the S1 pocket is solvent-exposed and less well-defined.^{29,37} As such, inhibitor analogues **3a** (R1 = ethyl) and **3b** (R1 = methyl) were synthesized to probe the relative contributions of the aliphatic *n*-butyl chain while reducing molecular weight and number of rotatable bonds of the inhibitor. While decreasing the R1 side chain to a methyl group resulted in a 13-fold decrease in potency, truncation to the smaller ethyl chain did not significantly affect the inhibitor potency (Table 2). Analysis of the separate binding constant K_i and rate constant for enzyme inactivation k_{inact} provided insight into how the structural changes are reflected in these values. The reduction in k_{inact}/K_i was largely a result of increases in the binding constant K_i with an approximate 15- and 2-fold increase for inhibitor **3a** and **3b**, respectively. Interestingly, the ethyl derivative **3a** was only slightly less potent despite a 2-fold decrease in binding affinity because the k_{inact} increased by almost 2-fold. The other sets of *n*-butyl and ethyl analogues, **3d/3e** and **3f/3g**, displayed the same trend: the ethyl derivatives had a slightly decreased binding affinity (higher K_i) and an enhanced k_{inact} resulting in approximately the same second-order rate constants k_{inact}/K_i .

Cruzain belongs to a family of enzymes where the interaction with the S2 pocket of the enzyme is the major specificity determinant.³⁰ The Connolly surface of the hydrophobic S2 pocket indicated that the isopropyl substituent in inhibitor **2** did not entirely fill the cavity. To take

Table 3. Evaluation of Efficacy and Toxicity of Inhibitors in Cell Culture

compd	<i>T. cruzi</i> IC ₅₀ (μM) ^b	host IC ₅₀ (μM) ^{a,b}
2	5.1	> 10
3a	8.3	> 10
3c	4.3	> 10
3d	3.1	> 10
3e	5.7	> 10
3f	4.1	> 10
3g	5.8	> 10
3h	4.2	10

^a *T. cruzi*-infected BESM cells. ^b Values are an average of duplicate or triplicate runs.

full advantage of the hydrophobic S2 pocket, a series of inhibitor analogues with increasingly larger R2 substituents were prepared. Replacement of the isopropyl group with the isobutyl group in inhibitor **3d** and the cyclobutyl group in inhibitor **3f** resulted in 4-fold improved potency with k_{inact}/K_i values of $657000 \text{ M}^{-1} \text{ s}^{-1}$ and $680000 \text{ M}^{-1} \text{ s}^{-1}$, respectively (Table 2). Not surprisingly, the increase in k_{inact}/K_i was a direct result of a 4-fold increase in the binding affinity (lower K_i) of these inhibitors for cruzain while the k_{inact} remained the same. Interestingly, inhibitor **3h** with a cyclopentyl substituent had a slightly lower k_{inact}/K_i due to a slight decrease in k_{inact} . The cyclohexyl substituent of inhibitor **3i** was too large, resulting in a dramatic increase in K_i and hence a drop in the overall second-order rate constant. These results are consistent with modeling studies, which indicated that the cyclobutyl and cyclopentyl ring were of optimal size, while the cyclohexyl ring was sterically hindered by close contacts with the S2 subsite. Inhibitor analogues combining optimal R1 and R2 substituents, **3e** (R1 = ethyl, R2 = isobutyl) and **3g** (R1 = ethyl, R2 = cyclobutyl), were also prepared and showed a 3-fold increase in potency.

Cell-Culture Evaluation of the Inhibitor Analogues. Tetrafluorophenoxymethyl ketone inhibitor **2** has previously been shown to completely eradicate the *T. cruzi* parasite in cell culture.¹⁷ Macrophages infected with *T. cruzi* were treated for 27 days with $10 \mu\text{M}$ inhibitor **2**, and cells were monitored for two more weeks to ensure complete elimination of the parasite. The more potent inhibitor analogues **3a** and **3c–h** were also evaluated for their effectiveness at eradicating the *T. cruzi* parasite in cell culture. For these analogues as well as inhibitor **2**, a new high through-put assay that provides IC₅₀ values as well as an evaluation of compound toxicity was employed.³⁸ In a 96-well plate, BESM cells infected with *T. cruzi* were incubated with several concentrations of the inhibitors (0, 0.3, 1, 3, and $10 \mu\text{M}$) for 3 days at 37°C . The wells were fixed and stained with a DNA fluorescent dye and then scanned with an automated fluorescence microscope. Host nuclei ($> 150 \mu\text{m}^2$) and parasite kinetoplast ($2–4 \mu\text{m}^2$) were differentiated based on size. A reduction of the number of *T. cruzi* per host cell provided a measure of parasite growth inhibition and a decrease in the number of host nuclei provided a quantitative measure of cytotoxicity.

All of the inhibitor analogues tested significantly decreased the number of intracellular parasites after the 3 day period of incubation as compared to untreated controls (Table 3). Curiously, even though the inhibitor derivatives **3a**, **3e**, and **3g** with R1 = ethyl had comparable second-order inactivation rates to their *n*-butyl counterparts (Table 2), they did not perform as well in cell culture. This is evidenced

in all three pairs of *n*-butyl/ethyl inhibitor analogues (Table 3: **2/3a**, **3d/3e**, and **3f/3g**). The more potent inhibitors **3d**, **3f**, and **3h** with R1 = *n*-butyl all had improved activity in cell culture (3.1–4.2 μM) compared to the first-generation inhibitor **2** (5.1 μM). Significantly, no apparent toxicity was observed: the host cell IC₅₀'s were greater than or equal to 10 μM for all of the tetrafluorophenoxymethyl ketone inhibitors.

Conclusion

The drugs available to treat Chagas disease are decades old and limited in efficacy.^{3,4} Validation of cruzain, the major cysteine protease of the *T. cruzi* parasite, as a target has provided an opportunity for developing improved chemotherapy.^{7–9} Proteases are a well-studied class of enzymes due to their involvement in many cellular processes and importance as targets for small-molecule therapeutics.³⁹ Peptidic inhibitors, consisting of small peptides coupled to an electrophilic pharmacophore, easily mimic the natural substrates of the protease and hence result in potent inhibitors. However, they do not possess the molecular properties required for drug candidates due to their susceptibility to hydrolysis, metabolism, and rapid clearance.^{16,40} To address this issue, we have developed a nonpeptidic class of triazole-based cruzain inhibitors.^{17,18}

In this study, nonpeptidic inhibitor **2** was evaluated in a mouse model of Chagas disease by twice daily dosing (20 mg/kg) via intraperitoneal injection for 27 days. After 77 days postinfection, visible signs of Chagas disease such as abdominal swelling, malaise, and weakness of the hind legs were not observed for the treated mice. The treatment was also well-tolerated with no apparent signs of toxicity. Additionally, two mice had negative hemocultures and displayed no signs of infection in heart tissue. For comparison, a similar treatment regime with the vinyl sulfone inhibitor **1** rescued animals from lethal infection at a higher daily dose (50 mg/kg).^{12,14} However, all of the treated mice did show some inflammation in skeletal muscle suggesting unresolved cryptic infection, which prompted the development of more potent inhibitors.

A high resolution crystal structure of inhibitor **2** complexed with cruzain was obtained. The structural information revealed how the triazole moiety of the inhibitor is able to provide the same stabilizing interactions with the enzyme active site as the amide bond in peptidic inhibitors. In addition to characterizing the binding mode of inhibitor **2**, the structure enabled the design of inhibitors with 4-fold increases in inhibitory activity and, for select inhibitors, improved physicochemical properties such as reduced molecular weight, lower hydrophobicity, and a reduction in the number of rotatable bonds. Several of these inhibitors also showed comparable or modestly improved potency relative to **2** in cell culture evaluation.

The tetrafluorophenoxymethyl ketone inhibitor **2** and the newly designed inhibitors **3** represent very promising drug leads for the treatment of Chagas disease. Evaluation of the pharmacokinetic properties of these compounds along with their evaluation in animal models of Chagas disease via oral administration is under active investigation.

Experimental Section

General Synthesis Methods. Unless otherwise noted, all reagents were obtained from commercial suppliers and used without purification. Tetrahydrofuran (THF), diethyl ether,

methylene chloride, and toluene were obtained from a Seca solvent system by GlassContour (solvent dried over alumina under an N₂ atmosphere). Anhydrous DMF (water < 50 ppm) was purchased from Acros. *p*-Toluenesulfonylmethylnitrosamide (Diazald) was purchased from Sigma-Aldrich. (*S*)-*tert*-Butanesulfinamide was provided by AllyChem Co. Ltd. (Dalian, China). Inhibitor **2** and intermediates **4a**, **5a**, and **7a** were synthesized as previously reported.¹⁷ Propargyl amines **6a–f** were synthesized according to reported procedures.⁴¹ All reactions were carried out in flame-dried glassware under an inert N₂ atmosphere. Normal-phase purification was carried out with Merck 60 230–240 mesh silica gel. Reverse-phase HPLC purification was conducted either with an Agilent 1100 series instrument or Biotage SP1 instrument (Charlottesville, VA) equipped with a Biotage C18SH column. Reverse-phase HPLC analysis was conducted with an Agilent 1100 series instrument. ¹H, ¹³C, ¹⁹F NMR spectra were obtained on a Bruker AV-300, AVB-400, AVQ-400, or DRX-500 at room temperature. Chemical shifts are reported in ppm, and coupling constants are reported in Hz. ¹H resonances are referenced to CHCl₃ (7.26 ppm) or DMSO-*d*₆ (4.90 ppm), ¹³C resonances are referenced to CHCl₃ (77.23 ppm) or DMSO-*d*₆ (39.50 ppm), and ¹⁹F resonances are referenced to CFC1₃ (0 ppm). Combustion analyses and high-resolution mass spectrometry analyses were performed by the University of California at Berkeley Microanalysis and Mass Spectrometry Facilities. All of the reported inhibitors displayed $\geq 95\%$ purity as determined by either combustion analysis or reverse-phase HPLC using two different solvent systems.

General Synthesis of 2,3,5,6-Tetrafluorophenoxymethyl Ketone Azides 5b–c (Procedure A). Step 1: This procedure was adapted from a prior publication.⁴² Isobutylchloroformate (1.1 equiv) was added to a 0.1 M solution of the azido acid⁴³ (1 equiv) and *N*-methyl morpholine (1.1 equiv) in THF at –40 °C. The reaction mixture was stirred for 20 min and then cannula filtered into a flask at 0 °C to remove the white solid. Excess diazomethane, prepared from Diazald (3.1 equiv), was introduced in situ according to the literature procedure⁴⁴ while the flask was maintained at 0 °C. After addition of the diazomethane, the reaction flask was stoppered and was maintained at 0 °C in a refrigerator overnight. The reaction mixture was treated with 48% aqueous HBr (3.8 equiv) and stirred for 15 min at 0 °C. After addition of the HBr, N₂ gas evolution was observed. The reaction mixture was diluted with EtOAc (50 mL) and was then washed with 10 wt % citric acid (2 \times 10 mL), saturated NaHCO₃ (2 \times 20 mL), and saturated NaCl (1 \times 10 mL). The organic layer was dried over Na₂SO₄, filtered, and concentrated under reduced pressure. Step 2: To a 0.6 M solution of 2,3,5,6-tetrafluorophenol (3.0–3.1 equiv) in DMF at 0 °C was added potassium fluoride (3.0 equiv), and the reaction mixture was stirred for 10 min. The appropriate bromomethyl ketone **4b** or **4c** (1.0 equiv) was then added in a small amount of DMF. The reaction mixture was stirred at 0 °C for 3 h. The reaction mixture was diluted with CH₂Cl₂ and washed with water (1 \times), saturated NaHCO₃ (1 \times), water (2 \times), and brine (1 \times). The organic layer was dried over Na₂SO₄, filtered, and concentrated under reduced pressure. The crude reaction mixture was purified by reverse-phase using 5–95% CH₃CN in H₂O with 0.1% CF₃CO₂H.

(S)-3-Azido-1-(2,3,5,6-tetrafluorophenoxy)pentan-2-one (5b). Procedure A, step 1, was followed using isobutylchloroformate (0.663 mL, 5.11 mmol), 2-azidobutyric acid (0.600 g, 4.65 mmol), *N*-methyl morpholine (0.562 mL, 5.11 mmol), Diazald (3.00 g, 13.95 mmol), and 48% aqueous HBr (1.05 mL) in THF (50 mL) to afford the crude product as a pale-yellow oil. Bromomethyl ketone **4b**, which is unstable, was taken on immediately without purification. ¹H NMR (300 MHz, CDCl₃): δ 1.05 (t, 3H, *J* = 7.4), 1.73–2.11 (m, 2H), 3.99–4.16 (m, 3H). Procedure A, step 2, was followed using bromomethyl ketone **4b** (0.480 g, 2.33 mmol), 2,3,5,6-tetrafluorophenol (1.16 g, 6.99

mmol), and potassium fluoride (0.406 g, 6.99 mmol) in DMF (7.0 mL) to afford 0.380 g (56%) of **5b** as a clear oil. ¹H NMR (400 MHz, CDCl₃): δ 1.07 (t, 3H, *J* = 7.4), 1.79–1.87 (m, 1H), 1.95–2.01 (m, 1H), 4.10 (dd, 1H, *J* = 4.9, 8.0), 5.00 (d, 1H, *J* = 17.5), 5.05 (d, 1H, *J* = 17.5), 6.78–6.85 (m, 1H). ¹³C NMR (100 MHz, CDCl₃): δ 10.1, 24.1, 66.9, 75.5 (t, *J* = 3.0), 99.9 (t, *J* = 23.0), 136.7–137.0 (m), 140.3 (dm, *J* = 246), 146.3 (dm, *J* = 246), 201.5. ¹⁹F NMR (376 MHz, CDCl₃): δ –156.4 to –156.2 (m, 2F), –138.4 to –138.3 (m, 2F). HRMS-FAB (*m/z*): [MLi]⁺ calcd for C₁₁H₉N₃O₂F₄Li, 298.0785; found, 298.0787.

(S)-3-Azido-1-(2,3,5,6-tetrafluorophenoxy)butan-2-one (5c). Procedure A, step 1, was followed using isobutylchloroformate (0.297 mL, 2.29 mmol), 2-azidopropionic acid (0.400 g, 2.08 mmol), *N*-methyl morpholine (0.251 mL, 2.29 mmol), Diazald (1.34 g, 6.24 mmol), and 48% aqueous HBr (0.47 mL) in THF (24 mL) to afford the crude product as a colorless oil. Bromomethyl ketone **4c**, which is unstable, was taken on immediately without purification. ¹H NMR (300 MHz, CDCl₃): δ 1.52 (d, 3H, *J* = 7.0), 3.91 (d, 1H, *J* = 7.0), 4.05 (d, 1H, *J* = 13.0), 4.12 (d, 1H, *J* = 13.0). Procedure A, step 2, was followed using bromomethyl ketone **4c** (0.17 g, 0.89 mmol), 2,3,5,6-tetrafluorophenol (0.442 g, 2.66 mmol), and potassium fluoride (0.155 g, 2.66 mmol) in DMF (2.2 mL) to afford 0.125 g (51%) of **5c** as a clear oil. ¹H NMR (400 MHz, CDCl₃): δ 1.54 (d, 3H, *J* = 7.1), 4.26 (q, 1H, *J* = 7.1), 5.03 (d, 1H, *J* = 17.7), 5.07 (d, 1H, *J* = 17.7), 6.78–6.85 (m, 1H). ¹³C NMR (100 MHz, CDCl₃): δ 15.3, 60.9, 75.0 (t, *J* = 3.0), 99.9 (t, *J* = 23.0), 136.8–136.9 (m), 140.3 (dm, *J* = 251), 146.3 (dm, *J* = 251), 201.6. ¹⁹F NMR (376 MHz, CDCl₃): δ –156.4 to –156.3 (m, 2F), –138.5 to –138.3 (m, 2F). HRMS-FAB (*m/z*): [MLi]⁺ calcd for C₁₀H₇N₃O₂F₄Li, 284.0629; found, 284.0631.

General Synthesis of Quinoline Propargyl Amines 7b–f (Procedure B). The HCl salt of propargyl amine **6b–f**⁴¹ (1.0–1.4 equiv) was dissolved in water and basified to pH = 11 with 1 M NaOH. The aqueous layer was then extracted with toluene (3×) and the organic layers were combined, dried over Na₂SO₄, and filtered to provide a 0.25 M solution of the volatile free-based amine **6b–f** in toluene. To the solution of propargyl amine **6b–f** were added quinoline-6-carboxyaldehyde (1–1.1 equiv) and activated 4 Å molecular sieves. The reaction mixture was stirred for 16 h and then filtered through a plug of celite. The celite was washed with CH₂Cl₂ (3×). The organic washes were combined and concentrated to afford the crude imine. To a 0.2 M solution of the propargyl imine (1 equiv) in methanol at 0 °C was added sodium borohydride (2 equiv). After stirring the reaction mixture at 0 °C for 1 h, it was diluted with water and extracted with CH₂Cl₂ (3×). The organic layers were combined, dried over Na₂SO₄, filtered, and concentrated. The crude reaction mixture was purified by silica-gel column chromatography (hexanes/ethyl acetate) to afford the pure product.

(S)-2-Cyclopropyl-*N*-(quinolin-6-ylmethyl)but-3-yn-2-amine (7b). Procedure B was followed using the HCl salt of propargyl amine **6b** (0.105 g, 0.720 mmol) and quinoline-6-carboxyaldehyde (0.113 g, 0.720 mmol) in toluene (3.0 mL), followed by reduction with sodium borohydride (0.054 g, 1.44 mmol) in methanol (4.0 mL) to afford 0.088 g (49%) of **7b** as a clear oil. ¹H NMR (400 MHz, CDCl₃): δ 0.41–0.50 (m, 3H), 0.61–0.66 (m, 1H), 0.99–1.06 (m, 1H), 1.53 (s, 3H), 2.32 (s, 1H), 4.03 (d, 1H, *J* = 12.8), 4.18 (d, 1H, *J* = 12.8), 7.39 (dd, 1H, *J* = 4.0, 8.4), 7.74 (dd, 1H, *J* = 2.0, 8.8), 7.81 (s, 1H), 8.06 (d, 1H, *J* = 8.8), 8.13 (d, 1H, *J* = 7.2), 8.89 (dd, 1H, *J* = 1.5, 4.4). ¹³C NMR (100 MHz, CDCl₃): δ 0.7, 2.6, 20.1, 28.7, 48.7, 56.2, 72.1, 84.2, 121.1, 126.3, 128.2, 129.4, 130.6, 135.8, 139.2, 147.7, 150.0.

(S)-3,5-Dimethyl-*N*-(quinolin-6-ylmethyl)hex-1-yn-3-amine (7c). Procedure B was followed using the HCl salt of propargyl amine **6c** (0.066 g, 0.41 mmol) and quinoline-6-carboxyaldehyde (0.048 g, 0.30 mmol) in toluene (1.6 mL), followed by reduction with sodium borohydride (0.023 g, 0.60 mmol) in methanol (1.5 mL) to afford 0.053 g (66%) of **7c**. ¹H NMR (400 MHz, CDCl₃): δ 1.00 (d, 6H, *J* = 6.8), 1.41 (s, 3H), 1.50–1.67 (m, 2H), 1.93

(sept, 1H, *J* = 6.5), 2.40 (s, 1H), 3.99 (d, 1H, *J* = 12.7), 4.06 (d, 1H, *J* = 12.7), 7.34 (dd, 1H, *J* = 4.3, 8.2), 7.71 (d, 1H, *J* = 8.8), 7.76 (s, 1H), 8.04 (d, 1H, *J* = 8.7), 8.08 (d, 1H, *J* = 8.4), 8.80–8.89 (m, 1H). ¹³C NMR (100 MHz, CDCl₃): δ 24.7, 24.80, 24.83, 27.7, 48.3, 50.5, 53.6, 71.5, 88.6, 121.3, 126.4, 128.4, 129.6, 130.7, 136.0, 139.4, 147.8, 150.2. HRMS-FAB (*m/z*): [MH]⁺ calcd for C₁₈H₂₃N₂, 267.1861; found, 267.1859.

(S)-2-Cyclobutyl-*N*-(quinolin-6-ylmethyl)but-3-yn-2-amine (7d). Procedure B was followed using the HCl salt of propargyl amine **6d** (0.111 g, 0.700 mmol) and quinoline-6-carboxyaldehyde (0.110 g, 0.700 mmol) in toluene (3.0 mL), followed by reduction with sodium borohydride (0.053 g, 1.400 mmol) in methanol (4.0 mL) to afford 0.115 g (63%) of **7d** as a clear oil. ¹H NMR (400 MHz, CDCl₃): δ 1.26 (s, 3H), 1.72–1.88 (m, 2H), 1.90–1.97 (m, 2H), 2.06–2.16 (m, 2H), 2.49 (s, 1H), 2.51–2.57 (m, 1H), 3.99 (d, 1H, *J* = 12.7), 4.06 (d, 1H, *J* = 12.7), 7.38 (dd, 1H, *J* = 4.2, 8.3), 7.72 (dd, 1H, *J* = 1.8, 8.7), 7.78 (s, 1H), 8.05 (d, 1H, *J* = 8.6), 8.12 (d, 1H, *J* = 7.9), 8.87 (dd, 1H, *J* = 1.5, 4.2). ¹³C NMR (100 MHz, CDCl₃): δ 17.1, 23.9, 24.0, 24.2, 44.9, 48.6, 57.2, 72.6, 86.2, 121.1, 126.3, 128.2, 129.4, 130.6, 135.8, 139.2, 147.6, 150.0. HRMS-ESI (*m/z*): [MH]⁺ calcd for C₁₈H₂₁N₂, 265.1699; found, 265.1706. Anal. Calcd for C₁₈H₂₀N₂: C, 81.78; H, 7.63; N, 10.60. Found: C, 81.50; H, 7.77; N, 10.59.

(S)-2-Cyclopentyl-*N*-(quinolin-6-ylmethyl)but-3-yn-2-amine (7e). Procedure B was followed using the HCl salt of propargyl amine **6e** (0.050 g, 0.29 mmol) and quinoline-6-carboxyaldehyde (0.050 g, 0.32 mmol) in toluene (1.2 mL), followed by reduction with sodium borohydride (0.022 g, 0.58 mmol) in methanol (1.5 mL) to afford 0.041 g (51%) of **7e** as a clear oil. ¹H NMR (400 MHz, CDCl₃): δ 1.39 (s, 3H), 1.50–1.62 (m, 4H), 1.64–1.75 (m, 2H), 1.79–1.86 (m, 2H), 2.08–2.13 (m, 1H), 2.36 (s, 1H), 3.99 (d, 1H, *J* = 12.8), 4.13 (d, 1H, *J* = 12.8), 7.38 (dd, 1H, *J* = 4.0, 8.0), 7.74 (dd, 1H, *J* = 2.0, 8.4), 7.79 (s, 1H), 8.06 (d, 1H, *J* = 8.4), 8.13 (d, 1H, *J* = 8.4), 8.88 (dd, 1H, *J* = 1.6, 4.4). ¹³C NMR (100 MHz, CDCl₃): δ 25.5, 25.8, 26.0, 27.8, 28.3, 48.4, 50.2, 57.5, 71.7, 87.0, 121.2, 126.3, 128.3, 129.6, 130.7, 135.9, 139.5, 147.8, 150.1. HRMS-ESI (*m/z*): [MH]⁺ calcd for C₁₉H₂₃N₂, 279.1856; found, 279.1859.

(S)-2-Cyclohexyl-*N*-(quinolin-6-ylmethyl)but-3-yn-2-amine (7f). Procedure B was followed using the HCl salt of propargyl amine **6f** (0.145 g, 0.92 mmol) and quinoline-6-carboxyaldehyde (0.129 g, 0.69 mmol) in toluene (2.8 mL), followed by reduction with sodium borohydride (0.052 g, 1.38 mmol) in methanol (3.4 mL) to afford 0.080 g (40%) of **7f**. ¹H NMR (300 MHz, CDCl₃): δ 1.03–1.31 (m, 5H), 1.33 (s, 3H), 1.48–1.58 (m, 1H), 1.63–1.72 (m, 1H), 1.76–1.87 (m, 2H), 1.92–2.05 (m, 2H), 2.39 (s, 1H), 4.01 (d, 1H, *J* = 12.6), 4.06 (d, 1H, *J* = 12.6), 7.38 (dd, 1H, *J* = 4.1, 8.1), 7.74 (dd, 1H, *J* = 2.1, 8.7), 7.79 (s, 1H), 8.05 (d, 1H, *J* = 8.7), 8.13 (d, 1H, *J* = 8.1), 8.88 (dd, 1H, *J* = 1.7, 4.3). ¹³C NMR (100 MHz, CDCl₃): δ 23.8, 26.75, 26.81, 26.9, 27.0, 28.2, 46.6, 48.2, 57.1, 71.6, 88.3, 121.3, 126.4, 128.4, 129.6, 130.8, 136.0, 139.6, 147.8, 150.2. HRMS-FAB (*m/z*): [MH]⁺ calcd for C₂₀H₂₅N₂, 293.2018; found, 293.2021.

General Synthesis of 2,3,5,6-Tetrafluorophenoxymethyl Ketone Inhibitors 3a–i (Procedure C). This procedure was adapted from Sharpless.⁴⁵ To a 0.25 M suspension of alkyne (1.0–1.2 equiv) and azide (1 equiv) in a 1:1 mixture of water and *tert*-butyl alcohol was added an aqueous solution of sodium ascorbate (1 equiv of a freshly prepared 1.0 M solution in water), followed by an aqueous solution copper(II) sulfate (0.1 equiv of a freshly prepared 0.3 M solution in water prepared from copper(II) sulfate pentahydrate). The heterogeneous mixture was stirred vigorously overnight. Water was added and extracted with EtOAc (3×). The organic layers were combined, washed with saturated NaCl (1×), dried over NaSO₄, filtered, and concentrated under reduced pressure. The crude reaction mixture was purified by HPLC [preparatory reverse-phase C₁₈ column (24.1 mm × 250 mm), CH₃CN/H₂O–0.1% CF₃CO₂H = 5:95 to 95:5 over 55 min; 10 mL/min; 254 nm detection for 65 min] and lyophilized to afford the CF₃CO₂H salt of the product. The free

amine of the product was obtained by dissolving the $\text{CF}_3\text{CO}_2\text{H}$ salt of the product in saturated aqueous NaHCO_3 and extracting with CH_2Cl_2 (4 \times). The organic layers were combined, dried over Na_2SO_4 , filtered, and concentrated under reduced pressure.

2,3,5,6-Tetrafluorophenoxyethyl Ketone Inhibitor 3a. Procedure C was followed using propargyl amine **7a** (0.030 g, 0.12 mmol), azide **5b** (0.032 g, 0.11 mmol), 1 M aqueous sodium ascorbate (0.024 g, 0.012 mmol), and 0.3 M aqueous copper(II) sulfate (0.003 g, 0.012 mmol) in 1:1 *t*BuOH:H₂O (0.5 mL) to afford 33.6 mg (52%) of a 1:1 mixture of diastereomers of **3a** as a pale-yellow oil. ¹H NMR (300 MHz, CDCl₃): δ 0.80 (d, 3H, *J* = 6.6), 0.93 (t, 1.5H, *J* = 7.5), 0.96 (t, 1.5H, *J* = 7.5), 1.02 (d, 3H, *J* = 6.6), 1.50 (s, 1.5H), 1.51 (s, 1.5H), 2.03–2.21 (m, 2H), 2.33–2.37 (m, 1H), 3.59 (d, 1H, *J* = 12.9), 3.77 (d, 1H, *J* = 12.9), 4.92 (s, 2H), 5.57 (dd, 1H, *J* = 5.1, 10.2), 6.73–6.85 (m, 1H), 7.37 (dd, 1H, *J* = 4.5, 8.4), 7.57 (s, 0.5H), 7.58 (s, 0.5H), 7.67–7.69 (m, 1H), 7.73 (s, 1H), 8.02 (d, 0.5H, *J* = 8.7), 8.03 (d, 0.5H, *J* = 8.7), 8.11 (m, 1H), 8.84–8.88 (m, 1H). ¹⁹F NMR (376 MHz, CDCl₃): δ -156.3 to -156.2 (m, 2F), -138.0 to -137.9 (m, 2F). HRMS-ESI (*m/z*): [MH]⁺ calcd for C₂₈H₃₀N₅O₂F₄, 544.2330; found, 544.2336. Anal. Calcd for C₂₈H₂₉N₅O₂F₄: C, 61.87; H, 5.38; N, 12.88. Found: C, 62.18; H, 5.40; N, 12.62.

2,3,5,6-Tetrafluorophenoxyethyl Ketone Inhibitor 3b. Procedure C was followed using propargyl amine **7a** (0.030 g, 0.12 mmol), azide **5c** (0.031 g, 0.11 mmol), 1 M aqueous sodium ascorbate (0.024 g, 0.12 mmol), and 0.3 M aqueous copper(II) sulfate (0.003 g, 0.012 mmol) in 1:1 *t*BuOH:H₂O (0.5 mL) to afford 27.1 mg (43%) of a 1:1 mixture of diastereomers of **3b** as a pale-yellow oil. ¹H NMR (300 MHz, CDCl₃): δ 0.81 (d, 3H, *J* = 6.9), 1.02 (d, 3H, *J* = 6.9), 1.51 (s, 3H), 1.84 (d, 1.5H, *J* = 5.1), 1.86 (d, 1.5H, *J* = 5.1), 2.17–2.22 (m, 1H), 3.61 (d, 1H, *J* = 12.9), 3.78 (d, 1H, *J* = 12.9), 4.87 (d, 1H, *J* = 16.8), 4.95 (d, 1H, *J* = 16.8), 5.74–5.80 (m, 1H), 6.73–6.84 (m, 1H), 7.37 (dd, 1H, *J* = 4.5, 8.4), 7.54 (s, 0.5H), 7.55 (s, 0.5H), 7.66–7.73 (m, 2H), 8.02 (d, 0.5H, *J* = 8.4), 8.04 (d, 0.5H, *J* = 8.4), 8.09–8.13 (m, 1H), 8.85–8.88 (m, 1H). ¹⁹F NMR (376 MHz, CDCl₃): δ -156.3 to -156.2 (m, 2F), -138.0 to -137.9 (m, 2F). HRMS-ESI (*m/z*): [MH]⁺ calcd for C₂₇H₂₈N₅O₂F₄, 530.2174; found, 530.2176. The purity of the inhibitor was determined by HPLC-MS analysis (C18 column (2.1 mm \times 150 mm); 0.4 mL/min; 254 nm detection in two solvent systems: CH₃CN/H₂O-0.1% CF₃CO₂H, 5:95 to 95:5 over 16 min, 95:5 for 2 min: 98%; CH₃OH/H₂O, 5:95 to 95:5 over 20 min, 95:5 for 10 min: 95%).

2,3,5,6-Tetrafluorophenoxyethyl Ketone Inhibitor 3c. Procedure C was followed using propargyl amine **7b** (0.030 g, 0.12 mmol), azide **5a** (0.032 g, 0.10 mmol), 1 M aqueous sodium ascorbate (0.024 g, 0.12 mmol), and 0.3 M aqueous copper(II) sulfate (0.003 g, 0.012 mmol) in 1:1 *t*BuOH:H₂O (0.5 mL) to afford 33.4 mg (49%) of a 1:1 mixture of diastereomers of **3c** as a pale-yellow oil. ¹H NMR (300 MHz, CDCl₃): δ 0.18–0.22 (m, 1H), 0.41–0.50 (m, 3H), 0.85 (t, 1.5H, *J* = 7.0), 0.87 (t, 1.5H, *J* = 7.0), 1.15–1.22 (m, 1H), 1.25–1.40 (m, 4H), 1.54 (s, 3H), 2.02–2.08 (m, 1H), 2.20–2.33 (m, 1H), 3.74 (d, 1H, *J* = 12.6), 3.87 (d, 1H, *J* = 12.6), 4.93 (s, 2H), 5.63–5.68 (m, 1H), 6.76–6.84 (m, 1H), 7.37 (dd, 1H, *J* = 4.5, 8.4), 7.61 (s, 0.5H), 7.62 (s, 0.5H), 7.65–7.70 (m, 1H), 7.73 (s, 1H), 8.02 (d, 0.5H, *J* = 8.4), 8.05 (d, 0.5H, *J* = 8.4), 8.09–8.13 (m, 1H), 8.84–8.88 (m, 1H). ¹⁹F NMR (376 MHz, CDCl₃): δ -156.2 to -156.1 (m, 2F), -138.0 to -137.9 (m, 2F). HRMS-ESI (*m/z*): [MH]⁺ calcd for C₃₀H₃₂N₅O₂F₄, 570.2492; found, 570.2488. Anal. Calcd for C₃₀H₃₁N₅O₂F₄: C, 63.26; H, 5.49; N, 12.30. Found: C, 62.93; H, 5.50; N, 11.90.

2,3,5,6-Tetrafluorophenoxyethyl Ketone Inhibitor 3d. Procedure C was followed using propargyl amine **7c** (0.017 g, 0.065 mmol), azide **5a** (0.021 g, 0.065 mmol), 1 M aqueous sodium ascorbate (0.065 mL, 0.065 mmol), and 0.3 M aqueous copper(II) sulfate (0.022 mL, 0.0065 mmol) in 1:1 *t*BuOH:H₂O (0.26 mL) to afford 30.0 mg (79%) of a 1:1 mixture of diastereomers of **3d** as a pale-yellow oil. ¹H NMR (400 MHz, CDCl₃): δ 0.760 (d,

1.5H, *J* = 6.6), 0.762 (d, 1.5H, *J* = 6.6), 0.83–0.92 (m, 6H), 1.09–1.23 (m, 1H), 1.23–1.45 (m, 3H), 1.61 (s, 1.5H), 1.62 (s, 1.5H), 1.68–1.80 (m, 2H), 1.82–1.88 (m, 2H), 1.98–2.12 (m, 1H), 2.24–2.36 (m, 1H), 3.61 (d, 0.5H, *J* = 12.6), 3.62 (d, 0.5H, *J* = 12.6), 3.76 (d, 1H, *J* = 12.6), 4.92 (s, 2H), 5.668 (dd, 0.5H, *J* = 4.7, 10.4), 5.673 (dd, 0.5H, *J* = 4.7, 10.4), 6.75–6.85 (m, 1H), 7.38 (dd, 1H, *J* = 4.3, 8.2), 7.59 (s, 0.5H), 7.60 (s, 0.5H), 7.64–7.69 (m, 1H), 7.72 (s, 1H), 8.02 (d, 0.5H, *J* = 8.7), 8.03 (d, 0.5H, *J* = 8.7), 8.09–8.14 (m, 1H), 8.85–8.89 (m, 1H). ¹⁹F NMR (376 MHz, CDCl₃): δ -156.2 to -156.0 (m, 2F), -138.0 to -137.8 (m, 2F). HRMS-FAB (*m/z*): [MH]⁺ calcd for C₃₁H₃₆N₅O₂F₄, 586.2796; found, 586.2805. Anal. Calcd for C₃₁H₃₅N₅O₂F₄: C, 63.58; H, 6.02; N, 11.96. Found: C, 63.53; H, 6.18; N, 11.96.

2,3,5,6-Tetrafluorophenoxyethyl Ketone Inhibitor 3e. Procedure C was followed using propargyl amine **7c** (0.018 g, 0.069 mmol), azide **5b** (0.020 g, 0.069 mmol), 1 M aqueous sodium ascorbate (0.069 mL, 0.069 mmol), and 0.3 M aqueous copper(II) sulfate (0.023 mL, 0.0069 mmol) in 1:1 *t*BuOH:H₂O (0.28 mL) to afford 26.0 mg (68%) of a 1:1 mixture of diastereomers of **3e** as a pale-yellow oil. ¹H NMR (400 MHz, CDCl₃): δ 0.76 (d, 3H, *J* = 6.6), 0.88–0.99 (m, 6H), 1.60 (br s, 1H), 1.61 (s, 1.5H), 1.62 (s, 1.5H), 1.70–1.80 (m, 1H), 1.82–1.88 (m, 2H), 2.04–2.15 (m, 1H), 2.30–2.42 (m, 1H), 3.62 (d, 1H, *J* = 12.7), 3.76 (d, 1H, *J* = 12.7), 4.93 (s, 2H), 5.68 (dd, 1H, *J* = 4.8, 10.3), 6.74–6.85 (m, 1H), 7.37 (dd, 1H, *J* = 4.1, 8.2), 7.59 (s, 0.5H), 7.60 (s, 0.5H), 7.64–7.66 (m, 0.5H), 7.66–7.69 (m, 0.5H), 7.72 (s, 1H), 8.02 (d, 0.5H, *J* = 8.7), 8.03 (d, 0.5H, *J* = 8.7), 8.09–8.14 (m, 1H), 8.84–8.90 (m, 1H). ¹⁹F NMR (376 MHz, CDCl₃): δ -156.2 to -156.1 (m, 2F), -138.0 to -137.9 (m, 2F). HRMS-FAB (*m/z*): [MH]⁺ calcd for C₂₉H₃₂N₅O₂F₄, 558.2485; found, 558.2487. Anal. Calcd for C₂₉H₃₁N₅O₂F₄: C, 62.47; H, 5.60; N, 12.56. Found: C, 62.37; H, 5.78; N, 12.35.

2,3,5,6-Tetrafluorophenoxyethyl Ketone Inhibitor 3f. Procedure C was followed using propargyl amine **7d** (0.023 g, 0.086 mmol), azide **5a** (0.027 g, 0.086 mmol), 1 M aqueous sodium ascorbate (0.086 mL, 0.086 mmol), and 0.3 M aqueous copper(II) sulfate (0.026 mL, 0.0086 mmol) in 1:1 *t*BuOH:H₂O (0.34 mL) to afford 25.7 mg (51%) of a 1:1 mixture of diastereomers of **3f** as a pale-yellow oil. ¹H NMR (400 MHz, CDCl₃): δ 0.84 (t, 1.5H, *J* = 7.2), 0.86 (t, 1.5H, *J* = 7.2), 1.09–1.23 (m, 1H), 1.23–1.45 (m, 4H), 1.537 (s, 1.5H), 1.542 (s, 1.5H), 1.67–2.00 (m, 7H), 2.00–2.14 (m, 1H), 2.24–2.37 (m, 1H), 2.81 (quint, 1H, *J* = 8.8), 3.63 (d, 1H, *J* = 12.8), 3.788 (d, 0.5H, *J* = 12.8), 3.794 (d, 0.5H, *J* = 12.8), 4.92 (s, 2H), 5.661 (dd, 0.5H, *J* = 4.8, 10.4), 5.665 (dd, 0.5H, *J* = 4.8, 10.4), 6.75–6.81 (m, 1H), 7.37 (dd, 1H, *J* = 4.2, 8.4), 7.58 (s, 0.5H), 7.59 (s, 0.5H), 7.686 (dd, 0.5H, *J* = 4.4, 8.8), 7.691 (dd, 0.5H, *J* = 4.4, 8.8), 7.74 (s, 1H), 8.02 (d, 0.5H, *J* = 8.8), 8.03 (d, 0.5H, *J* = 8.8), 8.09–8.14 (m, 1H), 8.84–8.89 (m, 1H). ¹⁹F NMR (376 MHz, CDCl₃): δ -156.2 to -156.1 (m, 2F), -138.0 to -137.9 (m, 2F). HRMS-ESI (*m/z*): [MH]⁺ calcd for C₃₁H₃₄N₅O₂F₄, 584.2643; found, 570.2649. The purity of the inhibitor was determined by HPLC-MS analysis (C18 column (2.1 mm \times 150 mm); 0.4 mL/min; 254 nm detection in two solvent systems: CH₃CN/H₂O-0.1% CF₃CO₂H, 5:95 to 95:5 over 16 min, 95:5 for 2 min: 99%; CH₃OH/H₂O, 5:95 to 95:5 over 20 min, 95:5 for 10 min: 96%).

2,3,5,6-Tetrafluorophenoxyethyl Ketone Inhibitor 3g. Procedure C was followed using propargyl amine **7d** (0.023 g, 0.086 mmol), azide **5b** (0.025 g, 0.086 mmol), 1 M aqueous sodium ascorbate (0.086 mL, 0.086 mmol), and 0.3 M aqueous copper(II) sulfate (0.026 mL, 0.0086 mmol) in 1:1 *t*BuOH:H₂O (0.34 mL) to afford 32.3 mg (68%) of a 1:1 mixture of diastereomers of **3g** as a clear oil. ¹H NMR (400 MHz, CDCl₃): δ 0.93 (t, 1.5H, *J* = 7.2), 0.95 (t, 1.5H, *J* = 7.2), 1.53 (s, 1.5H), 1.54 (s, 1.5H), 1.64–1.99 (m, 7H), 2.02–2.17 (m, 1H), 2.30–2.43 (m, 1H), 2.80 (quint, 1H, *J* = 8.8), 3.627 (d, 0.5H, *J* = 12.8), 3.631 (d, 0.5H, *J* = 12.8), 3.785 (d, 0.5H, *J* = 12.8), 3.788 (d, 0.5H, *J* = 12.8), 4.93 (s, 2H), 5.57 (dd, 0.5H, *J* = 4.8, 9.6), 5.58 (dd, 0.5H, *J* = 4.8, 9.6), 6.75–6.85 (m, 1H), 7.37 (dd, 1H, *J* = 4.4, 8.4), 7.58 (s, 0.5H), 7.59 (s, 0.5H), 7.688 (dd, 0.5H, *J* = 3.6, 8.6), 7.693 (dd, 0.5H,

$J=3.6, 8.6), 7.74 (s, 1H), 8.02 (d, 0.5H, J=8.6), 8.03 (d, 0.5H, J=8.6), 8.09-8.14 (m, 1H), 8.85-8.89 (m, 1H). ^{19}F NMR (376 MHz, CDCl_3): \delta -156.3 to -156.1 (m, 2F), -138.0 to -137.8 (m, 2F). MS (ESI): m/z 556 [MH]^+. Anal. Calcd for C_{29}H_{29}N_5O_2F_4: C, 62.69; H, 5.26; N, 12.61. Found: C, 62.27; H, 5.05; N, 12.29.$

2,3,5,6-Tetrafluorophenoxymethyl Ketone Inhibitor 3h. Procedure C was followed using propargyl amine **7e** (0.020 g, 0.072 mmol), azide **5a** (0.025 g, 0.079 mmol), 1 M aqueous sodium ascorbate (0.072 mL, 0.072 mmol), and 0.3 M aqueous copper(II) sulfate (0.022 mL, 0.0072 mmol) in 1:1 *t*BuOH:H₂O (0.29 mL) to afford 29.0 mg (67%) of a 1:1 mixture of diastereomers of **3h** as a pale-yellow oil. $^1H NMR (400 MHz, CDCl_3): \delta 0.85 (t, 1.5H, J = 7.2), 0.87 (t, 1.5H, J = 7.2), 1.08-1.22 (m, 1H), 1.22-1.53 (m, 9H), 1.57 (s, 1.5H), 1.58 (s, 1.5H), 1.64-1.81 (m, 3H), 1.99-2.12 (m, 1H), 2.23-2.35 (m, 1H), 2.42 (quint, 1H, J=8.8), 3.64 (d, 1H, J=12.8), 3.81 (d, 1H, J=12.8), 4.91 (s, 2H), 5.65 (dd, 1, J=4.8, 10.4), 6.76-6.84 (m, 1H), 7.38 (dd, 1H, J=4.0, 8.0), 7.58 (s, 0.5H), 7.59 (s, 0.5H), 7.69 (dd, 0.5H, J=4.4, 8.8), 7.70 (dd, 0.5H, J=4.4, 8.8), 7.74 (s, 1H), 8.02 (d, 0.5H, J=8.8), 8.03 (d, 0.5H, J=8.8), 8.08-8.14 (m, 1H), 8.83-8.89 (m, 1H). ^{19}F NMR (376 MHz, CDCl_3): \delta -156.2 to -156.0 (m, 2F), -138.0 to -137.8 (m, 2F). HRMS-ESI (m/z): [MH]^+ calcd for C_{32}H_{36}N_5O_2F_4, 598.2800; found, 598.2808. Anal. Calcd for C_{32}H_{35}N_5O_2F_4: C, 64.31; H, 5.90; N, 11.72. Found: C, 63.99; H, 6.15; N, 11.72.$

2,3,5,6-Tetrafluorophenoxymethyl Ketone Inhibitor 3i. Procedure C was followed using propargyl amine **7f** (0.024 g, 0.082 mmol), azide **5a** (0.026 g, 0.082 mmol), 1 M aqueous sodium ascorbate (0.082 mL, 0.082 mmol), and 0.3 M aqueous copper(II) sulfate (0.027 mL, 0.0082 mmol) in 1:1 *t*BuOH:H₂O (0.33 mL) to afford 33.5 mg (67%) of a 1:1 mixture of diastereomers of **3i** as a pale-yellow oil. $^1H NMR (400 MHz, CDCl_3): \delta 0.85 (t, 1.5H, J = 7.2), 0.87 (t, 1.5H, J = 7.2), 0.91-1.11 (m, 2H), 1.12-1.43 (m, 6H), 1.51 (s, 1.5H), 1.52 (s, 1.5H), 1.56-1.73 (m, 5H), 1.74-1.86 (m, 2H), 2.01-2.12 (m, 2H), 2.24-2.37 (m, 1H), 3.58 (d, 1H, J = 13.0), 3.77 (d, 1H, J = 13.0), 4.92 (s, 2H), 5.62-5.69 (m, 1H), 6.75-6.85 (m, 1H), 7.37 (dd, 1H, J = 4.2, 8.3), 7.55 (s, 0.5H), 7.56 (s, 0.5H), 7.65-7.70 (m, 1H), 7.72 (s, 1H), 8.01 (d, 0.5H, J=8.8), 8.02 (d, 0.5H, J=8.8), 8.09-8.14 (m, 1H), 8.85-8.89 (m, 1H). ^{19}F NMR (376 MHz, CDCl_3): \delta -156.2 to -156.1 (m, 2F), -138.0 to -137.9 (m, 2F). HRMS-FAB (m/z): [MH]^+ calcd for C_{33}H_{38}N_5O_2F_4, 612.2971; found, 612.2962. Anal. Calcd for C_{33}H_{37}N_5O_2F_4: C, 64.80; H, 6.10; N, 11.45. Found: C, 64.51; H, 6.46; N, 11.14.$

Cruzain Inhibition Assay. The k_{inact}/K_i for inhibitors were determined under pseudo-first-order conditions using the progress curve method.⁴⁶ The proteolytic cleavage of *N*-acyl aminocoumarins by cruzain was conducted in Dynatech Microfluor fluorescence 96-well microtiter plates. Assay wells contained a mixture of inhibitor and 1.0 μ M of Cbz-Phe-Arg-AMC ($K_m = 1.1 \mu$ M; purchased from Bachem) in buffer (100 mM solution of pH 6.3 sodium phosphate buffer with 400 mM of sodium chloride, 5 mM of DTT, 10 mM of EDTA, and 0.025% Triton-X 100). Aliquots of cruzain were added to each well to initiate the assay. The final enzyme concentration was 0.1 nM. Hydrolysis of the AMC substrate was monitored fluorometrically for 25 min using a Molecular Devices Spectra Max Gemini SX instrument. The excitation wavelength was 350 nm and the emission wavelength was 450 nm, with a cutoff of 435 nm. To determine the inhibition parameters, time points for which the control ($[I] = 0$) was linear were used. For each inhibitor, a k_{obs} was calculated for at least four different concentrations of inhibitors via a nonlinear regression of the data according to the equation $P = (v_i/k_{obs})[1 - \exp(-k_{obs}t)]$ (where product formation = P , initial rate = v_i , time = t , and the first-order rate constant = k_{obs}) using Prism 5 (GraphPad). For all inhibitors, k_{obs} varied hyperbolically with $[I]$ and nonlinear regression analysis was performed with Prism to determine k_{inact}/K_i using $k_{obs} = k_{inact}[I]/([I] + K_i*(1 + [S]/K_m))$. Inhibition was measured at

least in triplicate, and the average and standard deviation of the assays is reported.

***T. cruzi* Cell Culture Assay.** Mammalian cells were cultured in RPMI-1640 medium supplemented with 5% heat-inactivated fetal calf serum (FCS) at 37 °C in 5% CO₂. The Y strain of *T. cruzi* was maintained by serial passage in bovine embryo skeletal muscle (BESM) cells. Infectious trypomastigotes were collected from culture supernatants. A BESM cell suspension was dispensed into sterile 96-well black plates with clear bottom (Greiner Bio-One). Following cell attachment, cultures were infected with *T. cruzi* trypomastigotes. After infection, the culture medium was removed and replaced with 200 μ L of fresh culture medium containing several concentrations of the test inhibitors (0, 0.3, 1, 3, and 10 μ M). Culture plates were incubated for 72 h, washed once with PBS, and fixed for 2 h with 4% paraformaldehyde. Following a PBS wash to remove the fixative, host cell and parasite DNAs were labeled with 0.1 μ g/mL DAPI. Plates were kept in the dark at 4 °C until used for image acquisition by the IN Cell Analyzer 1000 imager (GE Healthcare) with a 10 \times objective. Ten image fields comprising 200–300 host cells were acquired per well. The IN Cell Workstation 3.5 multitarget analysis module was used for image analysis. Image segmentation parameters were set to identify host nuclei segmented with a minimum area of 150 μ m² and intracellular parasite nuclei with an area size of 2–4 μ m². Parasite nuclei/ host nuclei ratios were selected as measurement output and the average of duplicate or triplicate runs were used to generate IC₅₀ plots (Figure S1, Supporting Information).

Efficacy Studies in Mice. Female C3H mice (Jax) (mean weight 22 g; $n = 8$) were inoculated by intraperitoneal (ip) injection with 1.2×10^6 *T. cruzi* tissue culture trypomastigotes resuspended in 100 μ L of RPMI medium with 5% heat inactivated horse serum. Treatment ($n = 5$) was initiated 24 h post infection. A control group ($n = 3$) of similarly infected animals was left untreated. Compound **2** was resuspended daily in 100 μ L of 70% DMSO:30% ddH₂O, and injected b.i.d. via ip for 27 days at a dose of 20 mg/kg weight. Animals were sacrificed 77 days postinfection. Heart, skeletal muscle, liver, spleen, and colon were collected for histopathological studies. Blood (50 μ L) was collected by heart puncture and cultured in BHT medium at 27 °C. Hemocultures were maintained for 90 days and observed weekly for live parasites by contrast phase microscopy. Detailed histopathology and hemoculture results are listed in Table S1 (Supporting Information).

Crystallization and Data Collection. Cruzain was recombinantly expressed and purified (see Supporting Information for experimental details). Crystallization conditions were screened with the Mosquito drop-setting system (TTP Labtech) against a number of commercially available kits. Conditions yielding crystals (20% PEG 3000, 0.1 M sodium acetate pH 4.5) were reproduced in a 24-well format using 500 μ L of crystallization solution per well and hanging drops consisting of 1 μ L of protein and 1 μ L of well solution. Crystals were flash-cooled in well solution supplemented with 30% ethylene glycol and mounted in a cassette for the Stanford Auto Mounter (SAM) system.⁴⁷ Diffraction data were collected at the Stanford Synchrotron Radiation Lightsource (SSRL). Cruzain·**2** data were collected to 1.20 Å on BL7-1 at a temperature of 100 K and $\lambda = 0.98$ Å after selecting an optimal crystal from screening performed with the robotic SAM system. Reflections were indexed and integrated in the primitive monoclinic setting using MOSFLM⁴⁸ and scaled and merged in space group $P2_1$ with SCALA.⁴⁹ Intensities were then converted to structure factor amplitudes in TRUNCATE.⁵⁰ The cruzain·**2** structure was solved by molecular replacement in MOLREP⁵¹ using a high resolution structure of cruzain bound to a hydroxymethyl ketone inhibitor (PDB ID 1ME3). A single, clear rotation function solution was obtained at greater than 3 \times peak height/ σ of the second highest solution, suggesting one molecule of cruzain in the asymmetric unit. The translation function yielded a clear solution for the

monomer with a score of 0.67 and initial R_{work} of 34.6%. Rigid body refinement, followed by simulated annealing and grouped B factor refinement in CNS⁵² gave an R_{free} of 28.56% an R_{work} of 26.88% and yielded electron density maps of excellent quality. The inhibitor molecule was placed into $mF_o - DF_c$ difference electron density contoured at the 3σ level using COOT.⁵³ The resulting coordinates were refined through a combination of simulated annealing, positional, and isotropic B factor refinement in CNS. The model was completed by interspersing rounds of positional and anisotropic B factor refinement in REFMAC5⁵⁴ with manual adjustments in COOT. The structure has excellent stereochemistry, as determined by MOLPROBITY,⁵⁵ with 96.6% of residues in the favored regions, 100% in allowed regions, and no outliers. The final model contains 1 molecule of mature cruzain, 1 molecule of **2**, 265 water molecules, and 4 molecules of ethylene glycol. Statistics for data collection and refinement are given in Table S2 (Supporting Information). The coordinates and observed structure factors amplitudes for each model have been deposited in the Protein Data Bank under accession code 3IUT.

Acknowledgment. J.A.E. and K.B. gratefully acknowledge the NIH (GM0545051) for support of this work. K.B. greatly appreciates an American Chemical Society Division of Organic Chemistry Graduate Student Fellowship sponsored by Wyeth Pharmaceuticals. J.H.M., L.S.B., J.C.E., P.S.D., and I.D.K. gratefully acknowledge National Institutes of Health grant AI35707 and the Sandler Family Foundation for support of this work. Part of this research was performed at the Stanford Synchrotron Radiation Lightsource (SSRL), a national user facility operated by Stanford University on behalf of the U.S. Department of Energy, Office of Basic Energy Sciences. We thank Rafaela Ferreira for kindly providing the pPICZ α C construct with the cruzain insert. We also thank Clifford Bryant and Dr. Adam Renslo (Small Molecule Discovery Center, UCSF) for providing inhibitor **8** for kinetic analyses.

Supporting Information Available: *T. cruzi* cell culture IC₅₀ plots, detailed histopathology and hemoculture results, experimental details for the expression and purification of recombinant cruzain, and crystallographic data collection and refinement statistics. This material is available free of charge via the Internet at <http://pubs.acs.org>.

References

- Dias, J. C. Elimination of Chagas disease transmission: perspectives. *Mem. Inst. Oswaldo Cruz* **2009**, *104* (Suppl. I), 41–45.
- de Souza, W. Chagas' disease: facts and reality. *Microbes Infect.* **2007**, *9*, 544–545.
- Castro, J. A.; deMecca, M. M.; Bartel, L. C. Toxic side effects of drugs used to treat Chagas' disease (American Trypanosomiasis). *Human Exp. Toxicol.* **2006**, *25*, 471–479.
- Filardi, L. S.; Brener, Z. Susceptibility and natural resistance of *Trypanosoma cruzi* strains to drugs used clinically in Chagas' disease. *Trans. R. Soc. Trop. Med. Hyg.* **1987**, *81*, 755–759.
- Rodrigo, D.; Moreira, M.; Leite, A. C. L.; Ribeiro dos Santos, R.; Soares, M. B. P. Approaches for the development of new anti-*Trypanosoma cruzi* agents. *Curr. Drug Targets* **2009**, *10*, 212–231.
- Soeiro, M. N. C.; de Castro, S. L. *Trypanosoma cruzi* targets for new chemotherapeutic approaches. *Expert Opin. Ther. Targets* **2009**, *13*, 105–121.
- McKerrow, J. H.; Engel, J. C.; Caffrey, C. R. Cysteine protease inhibitors as chemotherapy for parasitic infections. *Bioorg. Med. Chem.* **1999**, *7*, 639–644.
- McKerrow, J. H.; McGrath, M. E.; Engel, J. C. The cysteine protease of *Trypanosoma cruzi* as a model for antiparasite drug design. *Parasitol. Today* **1995**, *11*, 279–282.
- Renslo, A. R.; McKerrow, J. H. Drug discovery and development for neglected parasitic diseases. *Nat. Chem. Biol.* **2006**, *2*, 701–710.
- Harth, G.; Andrews, N.; Mills, A. A.; Engel, J. C.; Smith, R.; McKerrow, J. H. Peptide-fluoromethyl ketones arrest intracellular replication and intercellular transmission of *Trypanosoma cruzi*. *Mol. Biochem. Parasitol.* **1993**, *58*, 17–24.
- Roush, W. R.; Gwaltney, S. L., II; Cheng, J.; Scheidt, K. A.; McKerrow, J. H.; Hansell, E. Vinyl sulfonate esters and vinyl sulfonamides: potent, irreversible inhibitors of cysteine proteases. *J. Am. Chem. Soc.* **1998**, *120*, 10994–10995.
- Engel, J. C.; Doyle, P. S.; Hsieh, I.; McKerrow, J. H. Cysteine protease inhibitors cure an experimental *Trypanosoma cruzi* infection. *J. Exp. Med.* **1998**, *188*, 725–734.
- Barr, S. C.; Warner, K. L.; Kornreic, B. G.; Piscitelli, J.; Wolfe, A.; Benet, L.; McKerrow, J. H. A cysteine protease inhibitor protects dogs from cardiac damage during infection by *Trypanosoma cruzi*. *Antimicrob. Agents Chemother.* **2005**, *49*, 5160–5161.
- Doyle, P. S.; Zhou, Y. M.; Engel, J. C.; McKerrow, J. H. A cysteine protease inhibitor cures Chagas' disease in an immunodeficient-mouse model of infection. *Antimicrob. Agents Chemother.* **2007**, *51*, 3932–3939.
- Jacobsen, W.; Christians, U.; Benet, L. Z. In vitro evaluation of the disposition of a novel cysteine protease inhibitor. *Drug Metab. Dispos.* **2000**, *28*, 1343–1351.
- Veber, D. F.; Johnson, S. R.; Cheng, H.-Y.; Smith, B. R.; Ward, K. W.; Kopple, K. D. Molecular properties that influence the oral bioavailability of drug candidates. *J. Med. Chem.* **2002**, *45*, 2615–2623.
- Brak, K.; Doyle, P. S.; McKerrow, J. H.; Ellman, J. A. Identification of a new class of nonpeptidic inhibitors of cruzain. *J. Am. Chem. Soc.* **2008**, *130*, 6404–6410.
- Brak, K.; Ellman, J. A. Nonpeptidic inhibitors of cruzain. WO patent application 2009/075778, **2009**.
- Krantz, A.; Copp, L. J.; Coles, P. J.; Smith, R. A.; Heard, S. B. Peptidyl (acyloxy)methyl ketones and the quiescent affinity label concept: the departing group as a variable structural element in the design of inactivators of cysteine proteinases. *Biochemistry* **1991**, *30*, 4678–4687.
- Smith, R. A.; Copp, L. J.; Coles, P. J.; Pauls, H. W.; Robinson, V. J.; Spencer, R. W.; Heard, S. B.; Krantz, A. New inhibitors of cysteine proteinases. Peptidyl acyloxymethyl ketones and the quiescent nucleofuge strategy. *J. Am. Chem. Soc.* **1988**, *110*, 4429–4431.
- Powers, J. C.; Aşgian, J. L.; Ekici, O. D.; James, K. E. Irreversible inhibitors of serine, cysteine, and threonine proteases. *Chem. Rev.* **2002**, *102*, 4639–4750.
- Baskin-Bey, E. S.; Washburn, K.; Feng, S.; Oltersdorf, T.; Shapiro, D.; Huyghe, M.; Burgart, L.; Garrity-Park, M.; van Vilsteren, F. G. I.; Oliver, L. K.; Rosen, C. B.; Gores, G. J. Clinical trial of the pan-caspase inhibitor, IDN-6556, in human liver preservation injury. *Am. J. Transplant.* **2007**, *7*, 218–225.
- Patterson, A. W.; Wood, W. J. L.; Hornsby, M.; Lesley, S.; Spraggon, G.; Ellman, J. A. Identification of selective, nonpeptidic nitrile inhibitors of cathepsin S using the substrate activity screening method. *J. Med. Chem.* **2006**, *49*, 6298–6307.
- Brady, K. D. Bimodal inhibition of caspase-1 by aryloxymethyl and acyloxymethyl ketones. *Biochemistry* **1998**, *37*, 8508–8515.
- Brady, K. D.; Giegel, D. A.; Grinnell, C.; Lunney, E.; Talianian, R. V.; Wong, W.; Walker, N. A catalytic mechanism for caspase-1 and for bimodal inhibition of caspase-1 by activated aspartic ketones. *Bioorg. Med. Chem.* **1999**, *7*, 621–631.
- Kerr, I. D.; Lee, J. H.; Farady, C. J.; Marion, R.; Rickert, M.; Sajid, M.; Pandey, K. C.; Caffrey, C. R.; Legac, J.; Hansell, E.; McKerrow, J. H.; Craik, C. S.; Rosenthal, P. J.; Brinen, L. S. Vinyl sulfones as antiparasitic agents and a structural basis for drug design. *J. Biol. Chem.* **2009**, *284*, 25697–25703.
- Brinen, L. S.; Hansell, E.; Cheng, J.; Roush, W. R.; McKerrow, J. H.; Fletterick, R. J. A target within a target: probing cruzain's P1' site to define structural determinants for the Chagas' disease protease. *Structure* **2000**, *8*, 831–840.
- Huang, L.; Brinen, L. S.; Ellman, J. A. Crystal structures of reversible ketone-based inhibitors of the cysteine protease cruzain. *Bioorg. Med. Chem.* **2003**, *11*, 21–29.
- McGrath, M. E.; Eakin, A. E.; Engel, J. C.; McKerrow, J. H.; Craik, C. S.; Fletterick, R. J. The crystal structure of cruzain: A therapeutic target for Chagas' disease. *J. Mol. Biol.* **1995**, *247*, 251–259.
- Gillmore, S. A.; Craik, C. S.; Fletterick, R. J. Structural determinants of specificity in the cysteine protease cruzain. *Protein Sci.* **1997**, *6*, 1603–1611.
- Angell, Y. L.; Burgess, K. Peptidomimetics via copper-catalyzed azide-alkyne cycloadditions. *Chem. Soc. Rev.* **2007**, *36*, 1674–1689.
- Brik, A.; Alexandratos, J.; Lin, Y.-C.; Elder, J. H.; Olson, A. J.; Wlodawer, A.; Goodsell, D. S.; Wong, C.-H. 1,2,3-Triazole as a

- peptide surrogate in the rapid synthesis of HIV-1 protease inhibitors. *ChemBioChem* **2005**, *6*, 1167–1169.
- (33) Horne, W. S.; Yadav, M. K.; Stout, C. D.; Ghadiri, M. R. Heterocyclic peptide backbone modifications in an α -helical coiled coil. *J. Am. Chem. Soc.* **2004**, *126*, 15366–15367.
- (34) Palmer, M. H.; Findlay, R. H.; Gaskell, A. J. Electronic charge distribution and moments of five- and six-membered heterocycles. *J. Chem. Soc., Perkin Trans. 2* **1974**, *4*, 420–428.
- (35) Kolb, H. C.; Sharpless, K. B. The growing impact of click chemistry on drug discovery. *Drug Discovery Today* **2003**, *8*, 1128–1137.
- (36) Bryant, C.; Kerr, I. D.; Debnath, M.; Ang, K. K. H.; Ratnam, J.; Ferreira, R. S.; Jaishankar, P.; Zhao, D.; Arkin, M. R.; McKerrow, J. H.; Brinen, L. S.; Renslo, A. R. Novel non-peptidic vinylsulfones targeting the S2 and S3 subsites of parasite cysteine proteases. *Bioorg. Med. Chem. Lett.* **2009**, *19*, 6218–6221.
- (37) Harris, J. L.; Backes, B. J.; Leonetti, F.; Mahrus, S.; Ellman, J. A.; Craik, C. S. Rapid and general profiling of protease specificity by using combinatorial fluorogenic substrate libraries. *Proc. Natl. Acad. Sci. U.S.A.* **2000**, *97*, 7754–7759.
- (38) McKerrow, J. H.; Doyle, P. S.; Podust, L. M.; Robertson, S. A.; Ferreira, R.; Saxton, T.; Arkin, M.; Kerr, I. D.; Brinen, L. S.; Craik, C. S. Two approaches to discovering and developing new drugs for Chagas disease. *Mem. Inst. Oswaldo Cruz* **2009**, *104* (Suppl. I), 263–269.
- (39) Abbenante, G.; Fairlie, D. P. Protease inhibitors in the clinic. *Med. Chem.* **2005**, *1*, 71–104.
- (40) Lipinski, C. A.; Lombardo, F.; Dominy, B. W.; Feeney, P. J. Experimental and computational approaches to estimate solubility and permeability in drug discovery and development settings. *Adv. Drug Delivery Rev.* **2001**, *46*, 3–26.
- (41) Patterson, A. W.; Ellman, J. A. Asymmetric synthesis of α,α -dibranched propargylamines by acetylide additions to *N*-tert-butanesulfinyl ketimines. *J. Org. Chem.* **2006**, *71*, 7110–7112.
- (42) Chino, M.; Wakao, M.; Ellman, J. A. Efficient method to prepare hydroxyethylamine-based aspartyl protease inhibitors with diverse P1 side chains. *Tetrahedron* **2002**, *58*, 6305–6310.
- (43) Pelletier, J. C.; Lundquist, J. T. Improved Solid-Phase Peptide Synthesis Method Utilizing α -Azide-Protected Amino Acids. *Org. Lett.* **2001**, *3*, 781–783.
- (44) Lombardi, P. A rapid, safe, and convenient procedure for the preparation and use of diazomethane. *Chem. Ind. (London)* **1990**, 708.
- (45) Rostovtsev, V. V.; Green, L. G.; Fokin, V. V.; Sharpless, K. B. A stepwise Huisgen cycloaddition process: copper(I)-catalyzed regio-selective “ligation” of azides and terminal alkynes. *Angew. Chem., Int. Ed.* **2002**, *41*, 2596–2599.
- (46) Bieth, J. G. Theoretical and practical aspects of proteinase inhibition kinetics. *Methods Enzymol.* **1995**, *248*, 59–84.
- (47) Cohen, A. E.; Ellis, P. J.; Deacon, A. M.; Miller, M. D.; Phizackerley, R. P. An automated system to mount cryo-cooled protein crystals on a synchrotron beamline, using compact sample cassettes and a small-scale robot. *J. Appl. Crystallogr.* **2002**, *35*, 720–726.
- (48) Leslie, A. G. W., Recent changes to the MOSFLM package for processing film and image plate data. *Joint CCP4 and ESF-EAMCB Newsletter on Protein Crystallography* **1992**, No. 26.
- (49) Evans, P. R. SCALA. *Joint CCP4 and ESF-EAMCB Newsletter on Protein Crystallography* **1997**, *33*, 22–24.
- (50) French, G. S.; Wilson, K. S. On the treatment of negative intensity observations. *Acta Crystallogr., Sect. A: Found. Crystallogr.* **1978**, *34*, 517–525.
- (51) Vagin, A.; Teplyakov, A. MOLREP: an automated program for molecular replacement. *J. Appl. Crystallogr.* **1997**, *30*, 1022–1025.
- (52) Brunger, A. T.; Adams, P. D.; Clore, G. M.; DeLano, W. L.; Gros, P.; Grosse-Kunstleve, R. W.; Jiang, J. S.; Kuszewski, J.; Nilges, M.; Pannu, N. S.; Read, R. J.; Rice, L. M.; Simonson, T.; Warren, G. L. Crystallography & NMR system: A new software suite for macromolecular structure determination. *Acta Crystallogr., Sect. D: Biol. Crystallogr.* **1998**, *54*, 905–921.
- (53) Emsley, P.; Cowtan, K. Coot: model-building tools for molecular graphics. *Acta Crystallogr., Sect. D: Biol. Crystallogr.* **2004**, *60*, 2126–2132.
- (54) Murshudov, G. N.; Vagin, A. A.; Dodson, E. J. Refinement of macromolecular structures by the maximum-likelihood method. *Acta Crystallogr., Sect. D: Biol. Crystallogr.* **1997**, *53*, 240–255.
- (55) Davis, I. W.; Leaver-Fay, A.; Chen, V. B.; Block, J. N.; Kapral, G. J.; Wang, X.; Murray, L. W.; W. Bryan Arendall, I.; Snoeyink, J.; Richardson, J. S.; Richardson, D. C. MolProbity: all-atom contacts and structure validation for proteins and nucleic acids. *Nucleic Acids Res.* **2007**, *35*, 1–9.